Hide-in-Motion: Embedding Steganographic Copyright Information into 4D Gaussian Splatting Assets

Hengyu Liu[1,†], Chenxin Li[1,†], Wentao Pan[1], Zhiqin Yang[1], Yifeng Yang[2], Yifan Liu[1], Wuyang Li[1], and Yixuan Yuan[1,*]

***Abstract*— As 4D extensions of 3D Gaussian Splatting (4D-GS) emerge as groundbreaking techniques for dynamic scene reconstruction and novel view synthesis in robotics and computer vision, ensuring the security and trustworthiness of these assets becomes crucial. While steganography has advanced significantly in 2D and 3D media, existing methods are inadequate for the complex, dynamic nature of 4D-GS representations. To address this gap, we propose Hide-in-Motion, a novel 4D steganography method for hiding information through deformation in Gaussian splatting. Our approach introduces a composite attribute and a Decouple Feature Field for coarse-to-fine deformation modeling and embedding implicit information, along with an Opacity-Guided Adaptive strategy. Hide-in-Motion overcomes the limitations of previous techniques, enhancing both the robustness of embedded information and the quality of 4D reconstruction. Extensive evaluations demonstrate that our method successfully embeds and recovers implicit information across various modalities while maintaining high rendering quality in dynamic scenes. This work not only advances copyright protection and secure data transmission for 4D assets but also paves the way for enhancing the security and integrity of 4D digital assets. Code is available at https://github.com/CUHK-AIM-Group/Hide-in-Motion.**

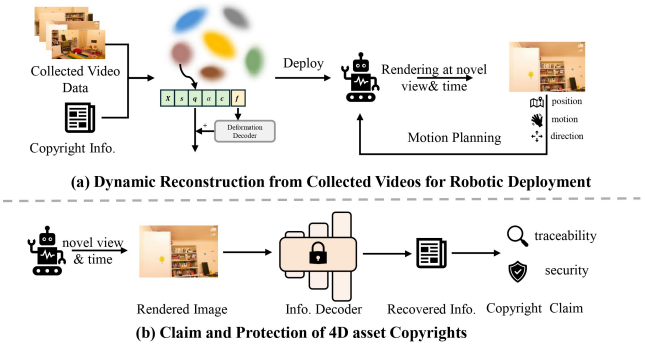

Fig. 1: **Typical Usage Case for Embedding Copyright into 4D assets**: (a) Dynamic reconstruction with the collect videos and deploy on robot, where robot makes motion planning with the rendering at novel view and timestamp; (b) Claim and protection of 4D assets copyrights, where we utilize the information recovered by an information decoder, traceability and security measures to safeguard 4D assets' copyrights.

I. INTRODUCTION

Novel View Synthesis (NVS) is a crucial task in computer vision and robotics, with wide applications in autonomous driving and augmented reality. 3D Gaussian Splatting (3D-GS)[1] has established itself as a prominent technique in 3D rendering, offering superior quality and fast rendering speeds. The 4D extensions of 3D-GS [2], [3], [4], [5], [6], [7] have demonstrated significant success in effectively reconstructing complex dynamic scenes. These advancements present unprecedented opportunities for enhancing robot training data. As shown in Fig. 1**(a)**, 4D Gaussian Splatting enables the generation of diverse, high-fidelity synthetic scenes that mimic real-world dynamics, significantly enhancing training data for robotic systems. This capability is invaluable when real-world data collection is challenging, dangerous, or ethically constrained. Efficient rendering and manipulation of these 4D scenes facilitate rapid generation of varied training scenarios, potentially accelerating learning and improving robotic model robustness across dynamic environments.

While 4D Gaussian assets hold immense value for robot training and deployment, their creation demands vast amounts of high-quality video data and significant computational resources, raising critical privacy and ownership concerns. These concerns underscore the importance of safeguarding the trained dynamic Gaussian models' intellectual property and confidentiality. As illustrated in Fig. 1**(b)**, our goal is to embed covert copyright information into these 4D assets, a stenographic pipeline which is essential for establishing trust in robotic learning systems. This approach creates a verifiable chain of trust from data creation to model deployment, ensuring data authenticity and integrity—critical for developing safe robotic systems while facilitating responsible data sharing. By addressing ethical concerns through embedded consent and usage restrictions, and concealing covert information in 4D assets, we not only protect intellectual property but also foster transparent, accountable robot training paradigms, ultimately contributing to trustworthy and ethically sound robotic systems.

Traditional steganography methods, whether in 2D or 3D, face significant limitations when applied to 4D representations. 2D techniques focusing on least significant bit manipulation or neural network-based decoding [8], [9], [10], [11] are inherently incompatible with the complex 3D and 4D

[1]Hengyu Liu, Chenxin Li, Wentao Pan, Zhiqin Yang, Yifan Liu, Wuyang Li and Yixuan Yuan are with the Department of Electronic Engineering, The Chinese University of Hong Kong, Hong Kong SAR, China, email: {piang.lhy@link.cuhk.edu.hk, yxyuan@ee.cuhk.edu.hk}.
[2]Yifeng Yang is with the School of Electronic Information and Electrical Engineering, Shanghai Jiao Tong University, Shanghai 200240, China.
This work was supported by Innovation and Technology Commission-Innovation and Technology Fund ITS/229/22 and Hong Kong Research Grants Council (RGC) General Research Fund 14220622.
† Equal Contribution, ∗ Corresponding Author.

rendering processes. Similarly, traditional 3D steganography methods employing Fourier and wavelet transforms [12], [13] require complete 3D model access and fail to address the dynamic nature of 4D-GS. Recent advancements in 3D steganography, such as StegaNeRF [14], CopyNeRF [15], and GS-hider [16], while innovative, present challenges when extended to 4D scenarios. Direct application of these methods to 4D-GS can result in prolonged training and rendering times, decreased rendering quality, or performance degradation due to the complex color modeling in dynamic scenes. Consequently, **existing 3D watermarking techniques are inadequate for 4D-GS, necessitating novel steganographic methods tailored to 4D Gaussian Splatting to ensure robust and efficient information hiding in these complex dynamic representations.**

To address these challenges, we propose **Hide-in-Motion** : a novel 4D steganography method. Building upon the dynamic modeling approach in [3], our method introduces an extra composite attribute and a set of deformation decoders for coarse-to-fine deformation modeling. We employ a Feature Gaussian Rasterizer to render a hidden feature map from the composite attribute of each hit Gaussian, which a private Hidden Decoder then processes to embed covert information within the deformation modeling attribute. Experimental results demonstrate that **Hide-in-Motion** effectively embeds information in Gaussian deformations while maintaining high rendering quality, with the private decoder successfully recovering hidden data with minimal impact on visual performance. Furthermore, our extended explorations reveal **Hide-in-Motion**'s versatility in embedding implicit information across various modalities, making it a robust solution for secure and trustworthy robot training data protection.

In short, our contributions are outlined as: (i) We pioneer the first steganographic method for 4D Gaussian Splatting assets, enabling imperceptible and recoverable information embedding in dynamic 4D representations for trustworthy robot training. (ii) We introduce a novel deformation-based information hiding technique using a composite attribute and Hidden Decoder system, ensuring robust embedding without compromising rendering quality. (iii) We propose a Decoupled Feature Field and Opacity-Guided Adaptive strategy to balance high-fidelity scene rendering and secure information embedding in 4D-GS representations. (iv) We validate our method through extensive experiments, demonstrating high recovery accuracy of embedded information while maintaining superior rendering quality in dynamic robotic training scenarios.

II. RELATED WORK

A. Implicit 3D Representations for Dynamic Reconstruction

Dynamic reconstruction methods [17], [18], [19], [20] based on Neural Radiance Fields (NeRF) [21] have been extensively explored, marking a significant advancement in the field of 3D scene representation and rendering. D-NeRF[17] uses a deformation network mapping scene deformations of each ray to a common canonical space and a canonical network for rendering. Nerfies[18] and HyperNeRF[19] use a trainable latent code to get the deformation of each frame. D^2NeRF [20] utilizes a composite radiance field to separately represent the dynamic objects and the static scene. These methods have shown remarkable ability to capture complex dynamic scenes, offering new possibilities for applications in robotics and computer vision. However, due to the repeated query of each ray when rendering, these NeRF-based methods suffer from slow rendering speed [22], limiting their practical applicability in real-time scenarios such as robotic navigation or augmented reality applications.

B. Explicit 3D Representations for Dynamic Reconstruction

4D extensions [4], [2], [6], [3], [5], [23], [24], [7] of 3D-GS [1], [25] have emerged with high rendering quality and rendering speed for dynamic reconstruction, addressing many of the limitations faced by implicit representations. D3DGS[4] use a deformation network to obtain the offset of dynamic Gaussians. 4DGaussian [2] utilizes the mutli-resolution Hexplanes [26] to store the spatial-temporal state of each Gaussian. STG [6] employs a collection of opacity features alongside a polynomial function to model deformation. E-D3DGS [3] introduces an additional attribute for each Gaussian and utilizes a network to capture both coarse and fine deformation aspects. These advancements in dynamic reconstruction not only improve rendering quality and speed but also offer promising potential for trustworthy robot training, where accurate and efficient representation of dynamic environments is crucial.

C. Steganography for 3D Representation

Steganography aims to embed hidden signals, such as images, videos, and text messages, within containers and to extract them accurately [27], [28], [29], [30], [31], [30]. Classic 3D steganography methods focus on using Fourier and wavelet transforms [12], [13] to hide information directly in explicit 3D representation (e.g. mesh). With the rise of NeRF and 3D-GS, steganography methods for novel 3D representations (NeRF and Gaussian) have emerged [14], [15], [16]. StegaNeRF [14] uses a classifier-guided strategy and finetune the pretrained model to encode watermark. CopyNeRF [15] use a watermarked color representation for encoding hidden message and distortion-resistant rendering for decoding. GS-Hider [16] replaces SH coefficients with a feature and recovers the rendering and hidden image from the splatted feature map. However, due to the complexity of 4D scenes, these methods fail to embed hidden information while ensuring the rendering quality.

III. METHODS

As shown in Fig. 2, the proposed steganography method **Hide-in-Motion** embeds implicit information into 4D assets. Deriving from the established principle of 3D-GS and the deformation modeling (Sec. III-A), we assign a composite attribute for each Gaussian, enabling information hiding in deformation (Sec. III-B). We utilize a decoupled feature field for dynamic scene rendering and implicit recovery (Sec. III-C). An Opacity-guided Adaptive Strategy is proposed in III-D to embed information in insignificant Gaussians.

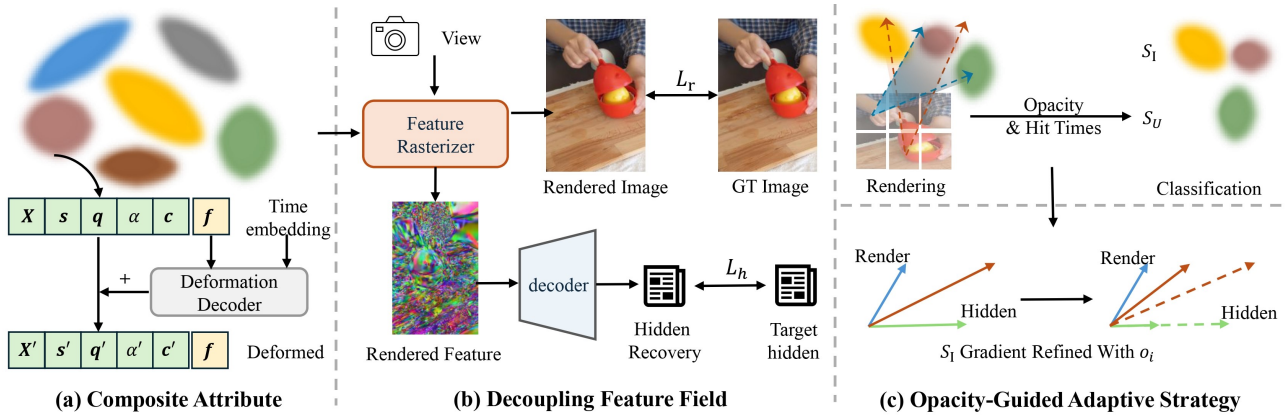

Fig. 2: Overview of **Hide-in-Motion**: (a) Steganographic Attributes in Deformation Modeling, by which a specialized composite attribute for each Gaussian serves for both invisible information embedding and deformation modeling; (b) Decoupled Feature Field for Steganographic Output, where a decoupled rendering design is used for simultaneously scene rendering and hidden information recovery; (c) Opacity-Guided Adaptive Strategy, which steers copyright information instilled in unimportant Gaussians, enhancing robustness while preserving visual quality.

A. Preliminaries of 4D Gaussian Splatting

3D Gaussian Splatting. 3D-GS [1] employs a collection of Gaussians with various attributes $\boldsymbol{G}_i = \{\boldsymbol{X}_i, \boldsymbol{s}_i, \boldsymbol{q}_i, \alpha_i, \boldsymbol{c}_i\}$ as 3D representation. $\boldsymbol{X} \in \mathbb{R}^3$ is the mean value of the Gaussian, scaling factor $\boldsymbol{s} \in \mathbb{R}^3$ and rotation quaternion $\boldsymbol{q} \in \mathbb{R}^4$ consists of the covariance matrix $\boldsymbol{\Sigma}$. $\alpha \in \mathbb{R}$ and $\boldsymbol{c} \in \mathbb{R}^C$ represent the opacity value and color feature, which are used for the view-independent color rendering:

$$\boldsymbol{C} = \sum_{i=1}^{N} \boldsymbol{c}_i \alpha_i \prod_{j=1}^{i-1} (1 - \alpha_i), \tag{1}$$

where N is the number of Gaussians. Gaussians are optimized to reconstruct the 3D scene through the differential splatting [32] and adaptive density control [1].

Lifting to 4D Gaussians via Deformation Modeling. Due to the higher rendering quality and efficiency, we use the strategy proposed in E-D3DGS [3] for deformation modeling. An extra attribute $\boldsymbol{z}_i$ is assigned for the given Gaussian to model the offsets of its attributes at each timestamp. Then two deformation decoders $\{\mathcal{D}_{\theta_c}, \mathcal{D}_{\theta_f}\}$ with $\boldsymbol{z}_i$ and time embedding of varying granularities are respectively used to regress the coarse deformation and fine deformation. The overall deformation is then calculated as the aggregate of the coarse and fine components.

B. Supercharging Steganographic Attributes into Deformation Modeling

In contrast to existing Gaussian Splatting methods with extra attributes [3], [33], [34], we introduce an innovative extra composite attribute $\boldsymbol{f} \in \mathbb{R}^M$ (M is the dimension of $\boldsymbol{f}$) for each Gaussian. This attribute is ingeniously designed to capture the dual concept of hiding information in deformation, essentially serving both deformation modeling and implicit information embedding. This dual-purpose approach not only enhances the security of embedded information but also maintains the integrity of the 4D representation, crucial for trustworthy robot training scenarios.

Following [3], **Hide-in-Motion** employs two coarse and fine deformation decoders $\{\mathcal{D}_{\theta_c}, \mathcal{D}_{\theta_f}\}$ for multi-granularity deformation modeling, where the decoder uses the composite feature $\boldsymbol{f}_i$ and time embedding of each granularity as input:

$$\Delta \boldsymbol{G}_i = \sum_{j \in \{c,f\}} \Delta \boldsymbol{G}_i^j, \text{ where } \Delta \boldsymbol{G}_i^j = \mathcal{D}_{\theta_j}(\boldsymbol{f}_i, \boldsymbol{\gamma}_j(t)), \tag{2}$$

where $j \in \{c, f\}$ denotes various granularities and $\boldsymbol{\gamma}_j(t)$ denotes the time embedding of corresponding granularity. The final deformed Gaussian at the given timestamp is represented as: $\boldsymbol{G}_i' = \{\boldsymbol{G}_i + \Delta \boldsymbol{G}_i, \boldsymbol{f}\}$.

Effectively, the interaction of composite attributes with implicit information embedding will be discussed in detail in Sec. III-C. It's important to note that simply removing $\boldsymbol{f}$ would cause **Hide-in-Motion** to lose its ability to model dynamic scenes effectively. This interdependence between the composite attribute and the dynamic scene modeling serves as an additional layer of security, making it extremely challenging for unauthorized parties to extract or manipulate the embedded information without compromising the entire 4D representation. Consequently, the Composite Attribute not only facilitates advanced deformation modeling but also effectively ensures the security and integrity of the embedded implicit information, aligning perfectly with the requirements for protecting the property rights and privacy of 4D assets.

C. Decoupling Feature Field for Steganographic Output

After deformation in the specified timestamp, **Hide-in-Motion** performs decoupled rendering for dynamic reconstruction and implicit information recovery. With the given viewpoint $\boldsymbol{P}$, **Hide-in-Motion** can get the rendered image $\boldsymbol{I}_{pred}$ with the deformed color feature and opacity in Eq. 1. As described in Eq. 3, we use L1 loss between the ground

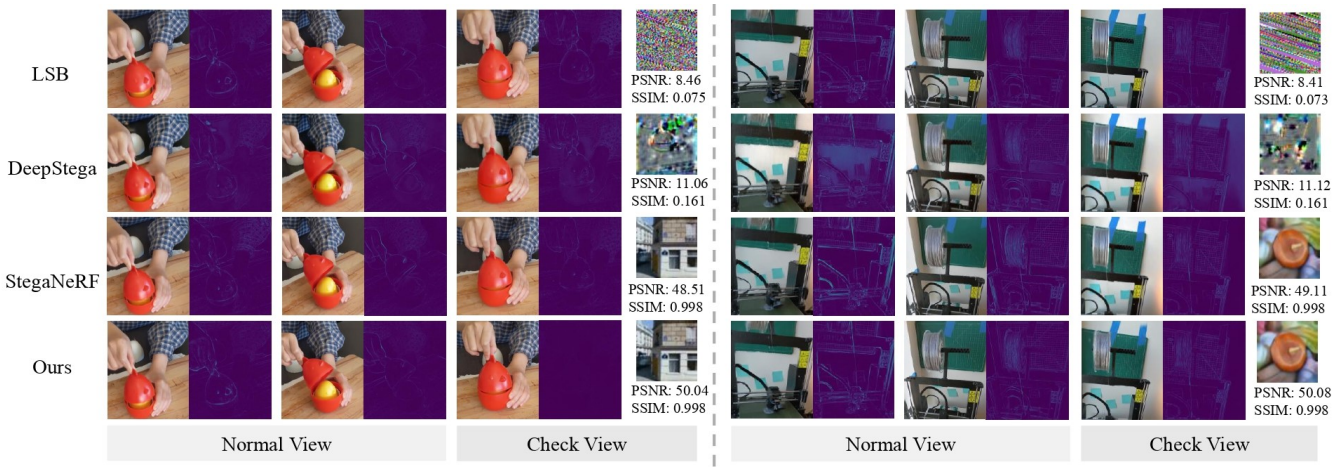

Fig. 3: Comparison of steganographic methods on HyperNeRF Dataset [19]: LSB, DeepStega, StegaNeRF, and our **Hide-in-Motion**. Each row shows rendered images and residual error with GT for normal and check views. Our method demonstrates superior visual quality and effective information hiding, evident from the contrast between normal and check view maps.

truth image $\boldsymbol{I}_{gt}$ and the predicted rendering $\boldsymbol{I}_{pred}$ to supervise the rendering process.

$$L_r = |\boldsymbol{I}_{pred} - \boldsymbol{I}_{gt}|. \tag{3}$$

While for the check viewpoint $\boldsymbol{P}_c$, where we intend to embed implicit information, **Hide-in-Motion** renders a composite feature map $\boldsymbol{F}$ containing implicit information from the composite attribute as described in Eq. 4,

$$\boldsymbol{F} = \sum_{i=1}^{N} \boldsymbol{f}_i \alpha_i \prod_{j=1}^{i-1}(1-\alpha_i). \tag{4}$$

To facilitate implicit information recovery, a decoder $\mathcal{D}_\theta$ is used for decoupling the implicit information $\boldsymbol{H}_{pred}$ from the composite feature map $\boldsymbol{F}$. Consistent with the approaches presented in [14], [16], **Hide-in-Motion** incorporates implicit information embedding through supervision during training.

$$\boldsymbol{H}_{pred} = \mathcal{D}_\theta(\boldsymbol{F}), \quad L_h^+ = |\boldsymbol{H}_{pred} - \boldsymbol{H}_{gt}|, \tag{5}$$

We utilize a invalid information to supervise the output of decoder on normal view $\boldsymbol{P}_n$ to prevent the decoder from overfitting the implicit information, which is referred as $\mathcal{L}_h^-$.

$$\mathcal{L}_h = \mathcal{L}_h^+ + \mathcal{L}_h^-, \quad \mathcal{L}_h^- = |\boldsymbol{H}_{pred} - \boldsymbol{H}_{invalid}|. \tag{6}$$

Consequently, this decoupling strategy allows **Hide-in-Motion** to embed hidden information in 4D Gaussian representations while preserving high-quality dynamic scene reconstruction. Our approach ensures the embedded data remains imperceptible in standard renderings while being recoverable from specific viewpoints (as the check viewpoint $\boldsymbol{P}_c$) [35]. This functionality supports both copyright and privacy protection effectively.

D. Instilling Ownership Information via Opacity-guided Adaptive Strategy

During the training process, thousands of Gaussians are employed to represent the 3D or 4D scene [1], [37]. However, there exists a considerable number of insignificant Gaussians, which either exhibit low opacity or are rarely 'hit' by rays from pixels during rendering. An intuitive idea is to embed the implicit information within the insignificant Gaussians. Driven by this insight and inspired by the global score utilized in [37], we propose our Opacity-Guided Implicit Embedding which intends to embed implicit information in insignificant Gaussians. Firstly, based on the opacity α and 'hit' times during rendering, we utilize an opacity-guided score o_i^t to metric the importance of the i-th Gaussian at timestamp t, which is shown in Eq. 7:

$$o_i^t = \sum_{h=1}^{H}\sum_{w=1}^{W} \mathbf{1}(\boldsymbol{G}_\mathbf{i}', \boldsymbol{p}_\mathbf{hw}, \mathbf{t}) \cdot \alpha_\mathbf{i} \cdot \mathbf{V}(\boldsymbol{s}_\mathbf{i}) \tag{7}$$

where the indicator function $\mathbf{1}(\boldsymbol{G}_\mathbf{i}', \boldsymbol{p}_\mathbf{hw}, \mathbf{t})$ denotes whether the pixel $\boldsymbol{p}_{hw}$ hits the i-th Gaussian at timestamp t and $V(\boldsymbol{s}) = 4\pi s_1 s_2 s_3/3$ represents the volume of Gaussian with the scale factor $\boldsymbol{s}$. With the calculated o_i^t for each Gaussian, we divide the Gaussians at time t into two sets: Important $S_I = \{i | i \geq h\}$ and Unimportant $S_U = \{i | i < h\}$, where h is the threshold for classification. To embed implicit information into S_U, we remove the gradients of S_I respected to L_h during the optimization process.

$$\frac{\partial \mathcal{L}}{\partial \boldsymbol{G}_i'} = \frac{\partial \mathcal{L}}{\partial \boldsymbol{G}_i'} - \frac{\partial \mathcal{L}_h}{\partial \boldsymbol{G}_i'}, \quad \forall i \in S_I. \tag{8}$$

Effectively, the derived opacity-guided strategy enhances the robustness of embedded information while minimizing impact on visual quality. By leveraging Gaussian representation characteristics, our approach seamlessly integrates ownership information, crucial for establishing trustworthy and verifiable 4D assets in robot training.

IV. EXPERIMENTS

A. Experimental Settings

Datasets. Following [3], [2], we utilize two widely recognized dynamic datasets: HyperNeRF Dataset [19] and Neural

Fig. 4: Qualitative results of dynamic reconstruction and implicit information embedding on Neural 3D Video Dataset [36]. Each row shows the rendering results of dynamic scenes and the recovered implicit information.

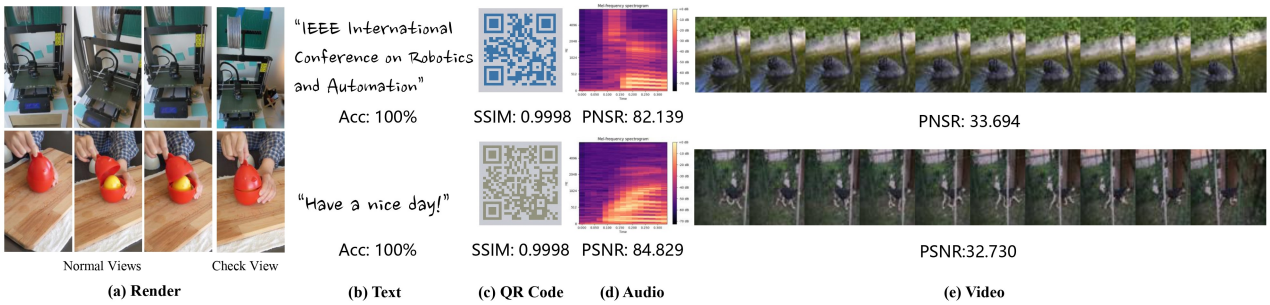

Fig. 5: Quantitative results of **Hide-in-Motion** with embedding implicit information of various modalities: (b) Text, (c) QR Code, (d) Audio and (e) Video. And (a) shows rendering results on both normal and check view when embedding audio.

3D Video Dataset [36]. For HyperNeRF Dataset [19], we utilize all frames of four scenes: *{Banana, Broom, Chicken, 3D-Printer}*. Neural 3D Video Dataset [36] has 20 multi-view videos with long duration and various movements. Following the setting in [3], we use six scenes of Neural 3D Video Dataset [36]: *{coffee_martini, cook_spinach, cut_roasted_beef, flame_salmon, flame_steak, sear_steak}*.

Metrics. Following [14], [30], [16], PSNR and SSIM are employed to measure the quality of recovered implicit information. Additionally, we utilize PSNR, SSIM, and LPIPS as metrics to evaluate the rendering quality of dynamic scenes. To evaluate the performance, we use four widely recognized techniques: LSB [38], DeepStega [10] and StegaNeRF [14] for comparison and we use these 3D steganography methods on 4D dynamic scenes reconstruction based on [3].

Implementation Details. For the main experiments, we use 2D images as target implicit information and follow the setting of [14], [30]. Data from other modalities as hidden information will be discussed in Sec. IV-D. A simple U-Net is utilized as the decoder for implicit information embedding [39]. The learning rate of the detector is set to $1e-4$ and the threshold h for Opacity-guided Adaptive Strategy is set to the 80% maximum value of the current pixels' scores. Other settings on HyperNeRF Dataset [19] and Neural 3D Video Dataset [36] as [3].

TABLE I: Quantitative Results of scene rendering and implicit information recovery on HyperNeRF Dataset [19]

Method	Dynamic Rendering			Implicit Recovery	
	PSNR↑	SSIM↑	LPIPS↓	PSNR↑	SSIM↑
E-D3DGS [3]	25.641	0.714	0.283	-	-
LSB [38]	24.956	0.688	0.323	8.436	0.075
DeepStega [10]	23.674	0.639	0.406	11.087	0.162
StegaNeRF [14]	25.099	0.688	0.332	48.508	**0.998**
Hide-in-Motion	**25.573**	**0.709**	**0.297**	**50.341**	**0.998**

B. Experimental Results

Experimental results on HyperNeRF Dataset [19] and Neural 3D Video Dataset [36] are respectively shown in Tab. I and Tab. II. We can observe that even traditional methods, such as LSB [38] and DeepStega [10], which are built upon dynamic Gaussian Splatting methods [3], still fail to effectively embed implicit information into 4D assets. LSB [38] and DeepStega [10] yield lower performance metrics, with PSNR values below 15 and SSIM scores

TABLE II: Quantitative Results of scene rendering and implicit information recovery on Neural 3D Video Dataset [36]

Method	Implicit Recovery			Watermark	
	PSNR↑	SSIM↑	LPIPS↓	PSNR↑	SSIM↑
E-D3DGS [3]	31.500	0.938	0.149	-	-
LSB [38]	30.721	0.925	0.158	8.647	0.083
DeepStega [10]	29.827	0.905	0.172	12.031	0.182
StegaNeRF [14]	30.615	0.923	0.163	47.432	0.995
Hide-in-Motion	**31.471**	**0.935**	**0.153**	**50.075**	**0.998**

under 0.20. This limitation adversely affects the overall performance of dynamic scene reconstruction, resulting in a decline of 0.6 to 1.9 in PSNR across both datasets. To bridge performance gap between the NeRF-based methods and Gaussian Splatting based methods, we employ a comparative approach built on [3] that adds hidden information with the strategy proposed in StegaNeRF [14]. While we find that directly using the steganography method proposed in [14] will lead to performance decline in dynamic reconstruction.

Visual results are shown in Fig. 3 and Fig. 4: LSB [38] and DeepStega [10] fail to recover the implicit information from the 4D assets, while StegaNeRF [14] has a performance decline on reconstruction. Compared to standard E-D3DGS model (without embedding implicit information), **Hide-in-Motion** only have a under 0.05 lower SSIM but a higher PSNR on both datasets, which indicates that **Hide-in-Motion** conceals the implicit information into 4D assets with almost no performance decline, thereby protecting the copyright property and privacy of 4D assets.

TABLE III: Ablation study of the components of **Hide-in-Motion** on HyperNeRF Dataset [19].

Method	Dynamic Rendering			Watermark	
	PSNR↑	SSIM↑	LPIPS↓	PSNR↑	SSIM↑
E-D3DGS	25.641	0.714	0.283	-	-
Hide-in-Motion	**25.573**	**0.709**	**0.297**	**50.341**	**0.998**
w.o. C.A.	25.103	0.689	0.318	49.935	**0.998**
w.o. D.R.	23.197	0.597	0.583	12.042	0.238
w.o. O.A.	25.059	0.703	0.311	50.274	**0.998**

C. Ablation Studies

To demonstrate the effectiveness of each component of our method, we perform ablation experiments on HyperNeRF Dataset [19]. The experimental results of the ablation study are presented in Table III. In this table, *w.o. C.A.* refers to a version of **Hide-in-Motion** that omits the composite attribute, relying solely on a decoder to recover implicit information. The *w.o. D.R.* condition illustrates the method rendering both the dynamic scene and implicit information from a decoupled feature map. *w.o. O.A.* represents **Hide-in-Motion** without the Opacity-guided Adaptive Strategy introduced in Sec. III-D. We can observe that the composite attribute supercharges the implicit information into deformation modeling. The results for *w.o. D.R.* indicates that when this additional attribute is employed for deformation modeling, implicit information embedding, and image rendering simultaneously, neither task can be fully learned. Therefore, the Decoupled Rendering Strategy is crucial for effectively embedding implicit information and accurate reconstruction. The performance decline observed in *w.o. O.A.* illustrates that the Opacity-guided Adaptive Strategy effectively embeds information within Gaussians with lower opacity and fewer occurrences of being hit during rendering. Overall, the main components of **Hide-in-Motion** are essential for embedding implicit information during dynamic reconstruction, thereby safeguarding the copyright of 4D assets.

D. Further Empirical Results

We further explore the capacity of **Hide-in-Motion** to embed implicit information from various modalities, including text, QR codes, audio, and video. In our implementation, we enhance the decoder by introducing modality-specific decoders tailored to each input type. This targeted approach allows for optimized performance across different forms of data. Following [30], we employ a range of metrics specific to each modality: accuracy for text; SSIM for QR code; PSNR for audio and video. The experimental results, illustrated in Fig. 5, unequivocally demonstrate that **Hide-in-Motion** effectively embeds a diverse array of implicit data modalities within 4D assets while achieving remarkable recovery performance. This advancement not only highlights the versatility of our approach but also paves the way for the practical application of steganographic techniques in copyright protection and secure data transmission related to 4D assets. By addressing the varied requirements of different data types, our method significantly contributes to enhancing the security and integrity of digital assets. Furthermore, our research investigates the performance of **Hide-in-Motion** under varying embedding capacities, demonstrating its scalability and potential to accommodate diverse steganographic requirements across different application scenarios, from lightweight watermarking to complex information hiding.

V. Conclusion

As dynamic reconstruction techniques utilizing Gaussian splatting gain prominence, the safeguarding of copyright and the security of 4D assets become paramount concerns. In this paper, we propose the first steganographic method **Hide-in-Motion** which efficiently embed implicit information in 4D assets through deformation modeling, with almost no performance decline of dynamic reconstruction. Our study illustrates that the exemplary performance of **Hide-in-Motion** is not only evident in both tasks but also extends to data across diverse modalities, thereby highlighting its effectiveness and versatility in a wide range of applications. This work not only enhances copyright protection and secure data transmission for 4D assets but also facilitates the development of reliable and verifiable robotic learning systems, highlighting the essential role of data provenance and integrity.

REFERENCES

[1] B. Kerbl, G. Kopanas, T. Leimkühler, and G. Drettakis, "3d gaussian splatting for real-time radiance field rendering," *TOG*, vol. 42, no. 4, pp. 1–14, 2023.

[2] G. Wu, T. Yi, J. Fang, L. Xie, X. Zhang, W. Wei, W. Liu, Q. Tian, and X. Wang, "4d gaussian splatting for real-time dynamic scene rendering," in *CVPR*, 2024, pp. 20 310–20 320.

[3] J. Bae, S. Kim, Y. Yun, H. Lee, G. Bang, and Y. Uh, "Per-gaussian embedding-based deformation for deformable 3d gaussian splatting," *arXiv preprint arXiv:2404.03613*, 2024.

[4] Z. Yang, X. Gao, W. Zhou, S. Jiao, Y. Zhang, and X. Jin, "Deformable 3d gaussians for high-fidelity monocular dynamic scene reconstruction," in *CVPR*, 2024, pp. 20 331–20 341.

[5] Y. Liu, C. Li, C. Yang, and Y. Yuan, "Endogaussian: Gaussian splatting for deformable surgical scene reconstruction," *arXiv preprint arXiv:2401.12561*, 2024.

[6] Z. Li, Z. Chen, Z. Li, and Y. Xu, "Spacetime gaussian feature splatting for real-time dynamic view synthesis," in *CVPR*, 2024, pp. 8508–8520.

[7] H. Liu, Y. Liu, C. Li, W. Li, and Y. Yuan, "Lgs: A light-weight 4d gaussian splatting for efficient surgical scene reconstruction," in *MICCAI*. Springer, 2024, pp. 660–670.

[8] A. A. Tamimi, A. M. Abdalla, and O. Al-Allaf, "Hiding an Image Inside Another Image Using Variable-Rate Steganography," *IJACSA*, vol. 4, no. 10, 2013.

[9] T. Pevnỳ, T. Filler, and P. Bas, "Using High-Dimensional Image Models to Perform Highly Undetectable Steganography," in *International Workshop on Information Hiding*, Springer. Springer, 2010, pp. 161–177.

[10] S. Baluja, "Hiding Images in Plain Sight: Deep Steganography," *NeurIPSs*, vol. 30, 2017.

[11] B. Shumeet, "Hiding images within images," *TPAMI*, vol. 42, no. 7, pp. 1685–1697, 2019.

[12] R. Ohbuchi, A. Mukaiyama, and S. Takahashi, "A frequency-domain approach to watermarking 3d shapes," in *Computer graphics forum*, vol. 21, no. 3. Wiley Online Library, 2002, pp. 373–382.

[13] Z. Wu, S. Song, A. Khosla, F. Yu, L. Zhang, X. Tang, and J. Xiao, "3d shapenets: A deep representation for volumetric shapes," in *CVPR*, 2015, pp. 1912–1920.

[14] C. Li, B. Y. Feng, Z. Fan, P. Pan, and Z. Wang, "Steganerf: Embedding invisible information within neural radiance fields," in *ICCV*, 2023, pp. 441–453.

[15] Z. Luo, Q. Guo, K. C. Cheung, S. See, and R. Wan, "Copyrnerf: Protecting the copyright of neural radiance fields," in *ICCV*, 2023, pp. 22 401–22 411.

[16] X. Zhang, J. Meng, R. Li, Z. Xu, Y. Zhang, and J. Zhang, "Gs-hider: Hiding messages into 3d gaussian splatting," *arXiv preprint arXiv:2405.15118*, 2024.

[17] A. Pumarola, E. Corona, G. Pons-Moll, and F. Moreno-Noguer, "D-nerf: Neural radiance fields for dynamic scenes," in *CVPR*, 2021, pp. 10 318–10 327.

[18] K. Park, U. Sinha, J. T. Barron, S. Bouaziz, D. B. Goldman, S. M. Seitz, and R. Martin-Brualla, "Nerfies: Deformable neural radiance fields," *ICCV*, 2021.

[19] K. Park, U. Sinha, P. Hedman, J. T. Barron, S. Bouaziz, D. B. Goldman, R. Martin-Brualla, and S. M. Seitz, "Hypernerf: A higher-dimensional representation for topologically varying neural radiance fields," *arXiv preprint arXiv:2106.13228*, 2021.

[20] T. Wu, F. Zhong, A. Tagliasacchi, F. Cole, and C. Oztireli, "Dˆ 2nerf: Self-supervised decoupling of dynamic and static objects from a monocular video," *NeurIPSs*, vol. 35, pp. 32 653–32 666, 2022.

[21] B. Mildenhall, P. P. Srinivasan, M. Tancik, J. T. Barron, R. Ramamoorthi, and R. Ng, "Nerf: Representing scenes as neural radiance fields for view synthesis," *Communications of the ACM*, vol. 65, no. 1, pp. 99–106, 2021.

[22] G. Chen and W. Wang, "A survey on 3d gaussian splatting," *arXiv preprint arXiv:2401.03890*, 2024.

[23] C. Li, B. Y. Feng, Y. Liu, H. Liu, C. Wang, W. Yu, and Y. Yuan, "Endosparse: Real-time sparse view synthesis of endoscopic scenes using gaussian splatting," in *MICCAI*. Springer, 2024, pp. 252–262.

[24] X. Liu, W. Li, T. Yamaguchi, Z. Geng, T. Tanaka, D. P. Tsai, and M. K. Chen, "Stereo vision meta-lens-assisted driving vision," *ACS Photonics*, vol. 11, no. 7, pp. 2546–2555, 2024.

[25] R. Li, Z. Fan, B. Wang, P. Wang, Z. Wang, and X. Wu, "Versatile-gaussian: Real-time neural rendering for versatile tasks using gaussian splatting," in *European Conference on Computer Vision*. Springer, 2024, pp. 258–275.

[26] A. Cao and J. Johnson, "Hexplane: A fast representation for dynamic scenes," in *CVPR*, 2023, pp. 130–141.

[27] X. Zhang, R. Li, J. Yu, Y. Xu, W. Li, and J. Zhang, "Editguard: Versatile image watermarking for tamper localization and copyright protection," in *CVPR*, 2024, pp. 11 964–11 974.

[28] G. C. Kessler and C. Hosmer, "An Overview of Steganography," *Advances in Computers*, vol. 83, pp. 51–107, 2011.

[29] X. Zhang, Y. Xu, R. Li, J. Yu, W. Li, Z. Xu, and J. Zhang, "V2a-mark: Versatile deep visual-audio watermarking for manipulation localization and copyright protection," in *ACM MM*, 2024, pp. 9818–9827.

[30] C. Li, H. Liu, Z. Fan, W. Li, Y. Liu, P. Pan, and Y. Yuan, "Gaussianstego: A generalizable stenography pipeline for generative 3d gaussians splatting," *arXiv preprint arXiv:2407.01301*, 2024.

[31] Y. Yang, H. Liu, C. Li, Y. Sun, W. Li, Y. Liu, Y. Lin, Y. Yuan, and N. Ye, "Concealgs: Concealing invisible copyright information in 3d gaussian splatting," *arXiv preprint arXiv:2501.03605*, 2025.

[32] W. Yifan, F. Serena, S. Wu, C. Öztireli, and O. Sorkine-Hornung, "Differentiable surface splatting for point-based geometry processing," *TOG*, vol. 38, no. 6, pp. 1–14, 2019.

[33] Z. Fan, J. Zhang, W. Cong, P. Wang, R. Li, K. Wen, S. Zhou, A. Kadambi, Z. Wang, D. Xu, *et al.*, "Large spatial model: End-to-end unposed images to semantic 3d," *arXiv preprint arXiv:2410.18956*, 2024.

[34] S. Zhou, H. Chang, S. Jiang, Z. Fan, Z. Zhu, D. Xu, P. Chari, S. You, Z. Wang, and A. Kadambi, "Feature 3dgs: Supercharging 3d gaussian splatting to enable distilled feature fields," in *CVPR*, 2024, pp. 21 676–21 685.

[35] P. Pan, Z. Fan, B. Y. Feng, P. Wang, C. Li, and Z. Wang, "Learning to estimate 6dof pose from limited data: A few-shot, generalizable approach using rgb images," in *3DV*. IEEE, 2024, pp. 1059–1071.

[36] T. Li, M. Slavcheva, M. Zollhoefer, S. Green, C. Lassner, C. Kim, T. Schmidt, S. Lovegrove, M. Goesele, R. Newcombe, *et al.*, "Neural 3d video synthesis from multi-view video," in *CVPR*, 2022, pp. 5521–5531.

[37] Z. Fan, K. Wang, K. Wen, Z. Zhu, D. Xu, and Z. Wang, "Lightgaussian: Unbounded 3d gaussian compression with 15x reduction and 200+ fps," *arXiv preprint arXiv:2311.17245*, 2023.

[38] C.-C. Chang, J.-Y. Hsiao, and C.-S. Chan, "Finding optimal least-significant-bit substitution in image hiding by dynamic programming strategy," *Pattern Recognition*, vol. 36, no. 7, pp. 1583–1595, 2003.

[39] O. Ronneberger, P. Fischer, and T. Brox, "U-net: Convolutional networks for biomedical image segmentation," in *MICCAI*, 2015, pp. 234–241.